A Physical Explanation for Natural Image Statistics

Jan-Mark Geusebroek and Arnold W. M. Smeulders

Abstract— **The statistics of texture operators on natural images are empirically determined to conform to a Weibull process. We explain these findings from the physical principles of fragmentation processes. The Weibull parameters are known to indicate the fractal dimension of the underlying system. Hence, we show the Weibull process to have a physical foundation for describing natural image statistics.**

Keywords— **Texture, Natural image statistics, Sequential fragmentation, Fractals.**

I. Introduction

An image typically consists of a million of pixels, each pixel being 1 value out of millions. Despite this overwhelming amount of choices to generate an image, there is a limited amount of configurations that represent a natural scene. In previous work, the effect of lighting conditions on the value of a pixel is investigated [1], resulting in local color invariance. From an analytical point of view this effectively separates scene accidental conditions from the true object characteristics. When seen from a reverse point of view, this constraints the probability of a pixel color by the light reflectance characteristics and the local coherence with neighboring pixels. In this paper, we investigate how spatial dependence influences the image formation process. Hence, we consider the statistical properties of local image structure.

Investigation of the statistics of natural images is an important topic for texture synthesis and recognition. Empirical studies [2], [3], [4] concentrate on the fitting of distributions to the response of linear operators for (large) sets of images. Empirical methods lack a physical basis, hence are difficult to interpret. The distributions determined are not easily proven to be the correct ones. Especially when the marginal statistics are considered important, as is often the case for reasoning in knowledge, finding the correct distribution is crucial.

Theoretical studies based on the statistics of surface reflectance properties include [5], [6], [7], [8]. These methods consider the physics of reflection to derive image statistics. Knowledge about the characteristics of the reflecting surface is explicitly assumed, for instance the slope distribution at the surface is Gaussian. Hence, there is a physical ground and a sufficient explanation of the parameters of the model. However, the model is only valid for a limited amount of natural images.

In this paper, we give a physical explanation for the statistics of local image structure of natural images. We start our analysis by introducing the Weibull distribution from the field of sequential fragmentation (Section II). The distribution originates from the study of particle distributions after milling. The Weibull distribution describes the number of particles as function of particle size or mass, hence the result of sieving processes. Section III gives an theoretical viewpoint on image derivative statistics. We confirm our findings by fitting the Weibull distribution to the histogram of derivative responses for the Curet database of natural textures [9], and discuss the implications.

Jan-Mark Geusebroek and Arnold W.M. Smeulders are with the Intelligent Sensory Information Systems, Informatics Institute, Faculty of Science, University of Amsterdam, Kruislaan 403, 1098 SJ Amsterdam, The Netherlands. Correspondence should be addressed to J.M.G. mark@science.uva.nl.

II. The Weibull Process

The Weibull process is derived from the particle number distribution $n(m)$, as given by Brown [10],

$$n(m) = c \int_m^\infty n(m') f(m' \to m)\, dm' \tag{1}$$

which indicates the number of fragments with mass between m and $m + dm$, contributed by fragmenting all particles of mass $m' > m$. The function $f(m' \to m)$ describes the mass distribution that results after fragmenting a heavy mass m'. The Weibull distribution results when assuming that small particles are more likely than larger particles to be the result of fragmentation. Hence, the fragmentation is a power-law process,

$$f(m' \to m) = \left(\frac{m}{m_1}\right)^\gamma, \quad -1 < \gamma \leq 0 \ . \tag{2}$$

Inserting Eq. (2) and solving Eq. (1) results in the Weibull probability density function [10],

$$n(m) = \frac{1}{m_1} \left(\frac{m}{m_1}\right)^\gamma e^{-\frac{1}{\gamma+1}\left(\frac{m}{m_1}\right)^{\gamma+1}} \tag{3}$$

where m_1 is related to the average mass, and γ the shape parameter, $-1 < \gamma \leq 0$. The integral form of the Weibull distribution given by

$$N(>m) \ = \ \int_m^\infty n(m)\, dm \ = \ e^{-\frac{1}{\gamma+1}\left(\frac{m}{m_1}\right)^{\gamma+1}} \tag{4}$$

indicates the total amount of particles of mass larger than m.

Equation (2) implies the Weibull distribution in particle mass. Conversion from mass to a size distribution is obtained by setting

$$\frac{m}{m_1} = \left(\frac{l}{l_1}\right)^3 \ . \tag{5}$$

Brown and Wohletz [11] theoretically derived the power-law process to describe the particle size distribution for the crushing of particles in a mill. Thereby providing a solid

physical basis for the distributions Eq. (3) and Eq. (4). They derived the parameter γ to be related to the fractal dimension D_f of the crushing process,

$$D_f = -3\gamma \tag{6}$$

where $0 \leq D_f < 3$ indicates the fractal dimension of the mass. As emphasized by Brown and Wohletz, the fractal dimension is a geometrical entity of a system [12].

III. Image Derivative Statistics

Local image structure is completely determined by the Taylor expansion of the image at a given point (x, y),

$$\hat{E}(x,y) = \hat{E} + \begin{pmatrix} x \\ y \end{pmatrix}^T \begin{bmatrix} \hat{E}_x \\ \hat{E}_y \end{bmatrix} + \frac{1}{2} \begin{pmatrix} x \\ y \end{pmatrix}^T \begin{bmatrix} \hat{E}_{xx} & \hat{E}_{xy} \\ \hat{E}_{xy} & \hat{E}_{yy} \end{bmatrix} \begin{pmatrix} x \\ y \end{pmatrix} + \dots \ . \tag{7}$$

The measurement is obtained by integrating over a certain spatial extent, the observation scale σ. Differentiation may be transported using Gaussian derivative filters,

$$\hat{E}_{x^n y^m}(x,y) = E(x,y) * G_{x^n y^m}(x,y;\sigma) \tag{8}$$

which results in the well-known N-Jet [13]. The coefficients of the Taylor expansion of $\hat{E}(x, y)$ together form a complete representation of the local image structure. Truncation of the Taylor expansion results in an approximate representation, the local equivalence class.

The respective statistics of each of the N-Jet components reflect the dependence between neighboring pixels. For the zeroth order measurement, the statistics are represented by the histogram of the Gaussian smoothed image intensity. The histogram is, neglecting smoothing effects, invariant under permutations of the pixels. Hence, the zeroth order statistics do not include joined statistics, and are irrelevant when considering pixel dependence.

Of considerable importance is the statistics of the first order derivatives,

$$\hat{E}_l \equiv \frac{\partial E}{\partial l} \quad \left[\frac{\text{intensity}}{\text{length}}\right] \tag{9}$$

where l indicates x or y. For construction of the response probability density function one takes a given response interval and sums over its spatial occurrences. When considering a unity step along the response $\partial \hat{E}_l$, one considers a certain variable distance ∂x in the spatial domain. This distance depends on the local image function $\hat{E}$.

As a result from scale-space theory, we consider that small details are occurring more often than large structures [14]. This is a direct implication of causality. Diffusion of numerous small structures will result in fewer large structures. Inversely, increasing magnification at large structures will resolve many smaller structures One may rephrase the statement in that, when resolving power increases, large structures will break-up into new structures, of which some of them are relatively large, but most of them will be small details. Hence, in one dimension, resolving a structure of length l into smaller structures yields a structure size distribution of

$$f(l' \to l) = \left(\frac{l}{l_1}\right)^{3\gamma} \tag{10}$$

where $l' \to l$ indicates the resolving of the structure l' into smaller structures of size l. The parameter l_1 is related to the average step size. The exponent 3γ includes the conversion Eq. (5) from size to mass. Equation (10) implies the Weibull distribution in length rather than mass.

Simoncelli [3] empirically found the generalized Laplacian,

$$P(c) = ze^{-\left|\frac{c}{s}\right|^p} \tag{11}$$

to fit to the marginal statistics of wavelet coefficients. Here, c indicates the wavelet coefficient, and s indicates the variance. The exponent p is related to γ in Eq. (4). The generalized Laplacian is the integral form Eq. (4) of the Weibull distribution. We have given a physical explanation for the empirical results as obtained by Simoncelli [3].

The Weibull shape parameter γ is related to the fractal dimension of the image as given by Eq. (6). Estimating γ from the histogram of image derivative responses indicates the fractal dimension of the image, as given by Eq. (6). Note that D_f is a strictly spatial property of an image. In conclusion, causality, the atlas principle, implies a Weibull distribution of structure size.

IV. Experiments

To give empirical evidence for our theory, we applied experiments on the Curet database of material textures [9]. For all 61 materials, we took a frontal view with arbitrary lighting direction, imaging setup number 42 from the 205 available per material. In this way, we could proceed with an automatic segmentation by selecting a rectangular material area from the images. We selected an area of 300 by 200 pixels from the center of the image. Horizontal Gaussian derivatives ($\sigma = 3$ pixels) were calculated over the material region, and a 256 bin histogram was constructed. The integral form of the Weibull distribution was fitted to the absolute value of the histogram, see Figure 1. The fitted shape parameter $\hat{\gamma}$, Eq. (4), was used to calculate the fractal dimension $D_f(x)$ Eq. (6) of the image. The experiment was repeated for the vertical derivative, and a measure of anisotropy was derived by considering the ratio between the horizontal and vertical fractal dimensions, $\Gamma = D_f(x)/D_f(y)$.

The results, together with the Kullback-Leibler divergence for goodness of fit are shown in Table I. The orange peel is not correctly segmented, and contains a black background area. Hence, the zero bin contains an disproportionally large value. The limestone and lettuce leaf histograms contain long tails with counts close to zero. Hence, the calculation of the Kullback-Leibler divergence becomes instable and deteriorates. The statistics of ribbed paper (x-direction), the corduroy (y-direction), and for the painted spheres (all directions), are the only materials for which the derivative response was clearly not Weibull distributed.

Note that these images consists mainly of regular texture. These represent a deliberately created texture, not an image of a chaotic process. This confirms our view, that most natural images are fractal in nature.

Note that the fractal dimension as derived from the histogram indeed estimates the spatial surface roughness, as can be derived by visual inspection of the materials, see Figure 2 and http://www.cs.columbia.edu/CAVE/curet/.

V. Discussion

We theoretically derived the statistics of local structure in natural images to follow a Weibull distribution. The derivation is explained from the physical principles of fragmentation processes. Thus we provide a physical explanation for the empirical results as obtained by Simoncelli [3].

We have shown that the fitting parameters estimated from Gaussian derivative response distributions indicate the fractal dimension, a strictly spatial property of an image. We demonstrated our point by experiments on the Curet database [9]. For 58 out of 61 images the Weibull distribution fitted well to the derivative statistics. As expected, the estimated fractal dimension indicates material surface roughness. The materials corduroy, ribbed paper, and painted spheres did not fit the Weibull distribution, as their structure is deliberately created to be highly regular.

The Weibull distribution arises when a scene is chaotic at all scales. A large class of natural scenes are fractal [12]. Hence, these images fulfill the property that more detail is added while zooming in. This causality, the atlas principle, implies a Weibull distribution of structure size.

The dual process of fragmentation is sieving. Nature "applies" sequential fragmentation of structures to refine a scene. Measurement involves the sieving of the scene to sort out the structures present. Since both processes are dual, one can make no distinction between fragmentation or sieving from the final result. Hence, sieving an image with arbitrary mesh size will result in a Weibull distribution for the local statistics. Scale-space filtering [14] is considered to be the sieving process dual to resolving power. The choice of the mesh size, hence the filter scale, will not affect the statistical result, except for a reparameterization.

We intent to use the Weibull distribution to parameterize local image structure in large pictorial databases. Similarity between images may now be expressed by similarity between the Weibull parameters, accelerating retrieval performance. Future research include the assesment of geometric and photometric invariant properties from the Weibull model.

TABLE I

Fitting results for the Curet dataset.

Material	KL	γ	Γ	$D_f(x)$
Peacock Feather	0.0271	-0.76	1.03	2.28
Sponge	0.0551	-0.66	1.06	1.99
Moss	0.0434	-0.65	1.05	1.96
Aluminum Foil	0.0015	-0.59	0.99	1.77
Limestone	0.1501	-0.59	0.96	1.76
Orange Peel	0.6233	-0.57	1.03	1.72
Lettuce Leaf	0.2151	-0.55	0.92	1.66
Insulation	0.0420	-0.53	1.02	1.60
Straw	0.0432	-0.52	1.15	1.57
Soleirolia Plant	0.0166	-0.52	0.93	1.56
Cracker b	0.0714	-0.51	0.96	1.54
Concrete c	0.0008	-0.51	1.06	1.52
Roof Shingle zoomed	0.0253	-0.50	0.87	1.51
Wood a	0.0288	-0.50	1.17	1.51
Crumpled Paper	0.0134	-0.50	0.97	1.49
Roof Shingle	0.0130	-0.49	0.98	1.46
Salt Crystals	0.0056	-0.48	1.01	1.45
White Bread	0.0563	-0.48	0.99	1.45
Plaster b zoomed	0.0116	-0.47	1.11	1.41
Tree Bark	0.0490	-0.47	0.93	1.40
Corn Husk	0.0356	-0.46	1.22	1.38
Artificial Grass	0.0005	-0.44	0.97	1.32
Styrofoam	0.0426	-0.44	0.96	1.32
Leather	0.0105	-0.44	0.87	1.31
Cracker a	0.0087	-0.43	1.18	1.30
Slate b	0.0296	-0.43	0.91	1.29
Slate a	0.0504	-0.43	0.91	1.28
Human Skin	0.0366	-0.43	0.96	1.28
Rug b	0.0075	-0.42	0.92	1.26
Lambswool	0.0103	-0.42	1.09	1.26
Felt	0.0025	-0.42	1.10	1.25
Rough Tile	0.0151	-0.42	0.94	1.25
Rabbit Fur	0.0034	-0.42	1.21	1.25
Stones	0.0016	-0.42	0.94	1.25
Terrycloth	0.0174	-0.41	0.96	1.24
Plaster b	0.0035	-0.41	0.92	1.22
Rough Paper	0.0003	-0.41	1.27	1.22
Loofa	0.0056	-0.40	1.09	1.20
Concrete b	0.0131	-0.40	0.99	1.20
Brown Bread	0.0124	-0.39	0.89	1.17
Linen	0.0130	-0.39	1.00	1.16
Wood b	0.0091	-0.39	0.95	1.16
Brick b	0.0421	-0.38	0.80	1.15
Polyester	0.0049	-0.38	1.03	1.14
Quarry Tile	0.0090	-0.37	0.99	1.11
Corduroy	0.0048	-0.37	-2.47	1.11
Frosted Glass	0.0112	-0.36	0.90	1.09
Concrete a	0.0531	-0.36	0.74	1.08
Cotton	0.0051	-0.36	3.72	1.08
Cork	0.0089	-0.35	0.87	1.06
Brick a	0.0072	-0.35	0.89	1.06
Pebbles	0.0009	-0.34	0.87	1.03
Polyester zoomed	0.0127	-0.34	0.86	1.01
Velvet	0.0099	-0.33	0.81	1.00
Plaster a	0.0029	-0.33	0.88	0.99
Rug a	0.0001	-0.33	0.85	0.99
Sandpaper	0.0050	-0.32	0.83	0.97
Rough Paper zoomed	0.0023	-0.30	0.75	0.90
Rough Plastic	0.0098	-0.26	0.59	0.79
Painted Spheres	0.0415	-0.05	0.12	0.14
Ribbed Paper	0.1235	14.89	-31.01	-44.66

For each material, the Kullback-Leibler divergence (KL), the Weibull exponent γ, the anisotropy $\Gamma = D_f(x)/D_f(y)$, and the horizontal fractal dimension $D_f(x)$ are given. Results are sorted by fractal dimension $D_f(x)$.

References

[1] J. M. Geusebroek, R. van den Boomgaard, A. W. M. Smeulders, and H. Geerts, "Color invariance," *IEEE Trans. Pattern Anal. Machine Intell.*, vol. 23, no. 12, pp. 1338–1350, 2001.

[2] J. M. Jolion, "Image and the benford's law," *J. Math. Imaging Vision*, vol. 14, pp. 73–81, 2001.

[3] E. P. Simoncelli, "Modeling the joint statistics of images in the wavelet domain," in *Proc. SPIE*. 1999, vol. 3813, pp. 188–195, SPIE.

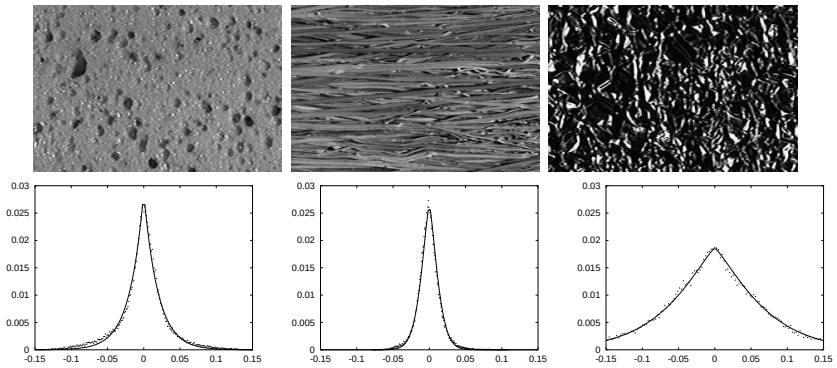

Fig. 1. The sponge, straw, and aluminum foil images from the Curet dataset [9]. The sponge edges are mainly caused by shadow. The straw is highly anisotropic, and edge detection is performed along its dominant orientation. Edges in the aluminum foil are caused by specular reflectance. The derivative histograms for each image and the fitting to a Weibull distribution are shown.

[4] J.H. van Hateren and A. van der Schaaf, "Independent component filters of natural images compared with simple cells in primary visual cortex," *Proc. R. Soc. Lond. B*, vol. 265, pp. 359–366, 1998.

[5] K. J. Dana and S. K. Nayar, "Histogram model for 3d textures," in *Proc. CVPR*. 1998, IEEE Computer Society.

[6] J. J. Koenderink and A. J. van Doorn, "Illuminance texture due to surface mesostructure," *J. Opt. Soc. Am. A*, vol. 13, no. 3, pp. 452–463, 1996.

[7] J. J. Koenderink, A. J. van Doorn, K. J. Dana, and S. Nayar, "Bidirectional reflection distribution function of thoroughly pitted surfaces," *Int. J. Comput. Vision*, vol. 31, pp. 129–144, 1999.

[8] B. van Ginneken and J. J. Koenderink, "Texture histograms as a function of irradiation and viewing direction," *Int. J. Comput. Vision*, vol. 31, pp. 169–184, 1999.

[9] K. J. Dana, B. van Ginneken, S. K. Nayar, and J. J. Koenderink, "Reflectance and texture of real world surfaces," *ACM Trans Graphics*, vol. 18, pp. 1–34, 1999.

[10] W. K. Brown, "A theory of sequential fragmentation and its astronomical applications," *J. Astrophys. Astr.*, vol. 10, pp. 89–112, 1989.

[11] W. K. Brown and K. H. Wohletz, "Derivation of the weibull distribution based on physical principles and its connection to the rosin-rammler and lognormal distributions," *J. Appl. Phys.*, vol. 78, pp. 2758–2763, 1995.

[12] B. B. Mandelbrot, *The Fractal Geometry of Nature*, W. H. Freeman and Co., New York, NY, 1983.

[13] L. M. J. Florack, B. M. ter Haar Romeny, J. J. Koenderink, and M. A. Viergever, "Scale and the differential structure of images," *Image Vision Comput.*, vol. 10, no. 6, pp. 376–388, 1992.

[14] J. J. Koenderink, "The structure of images," *Biol. Cybern.*, vol. 50, pp. 363–370, 1984.

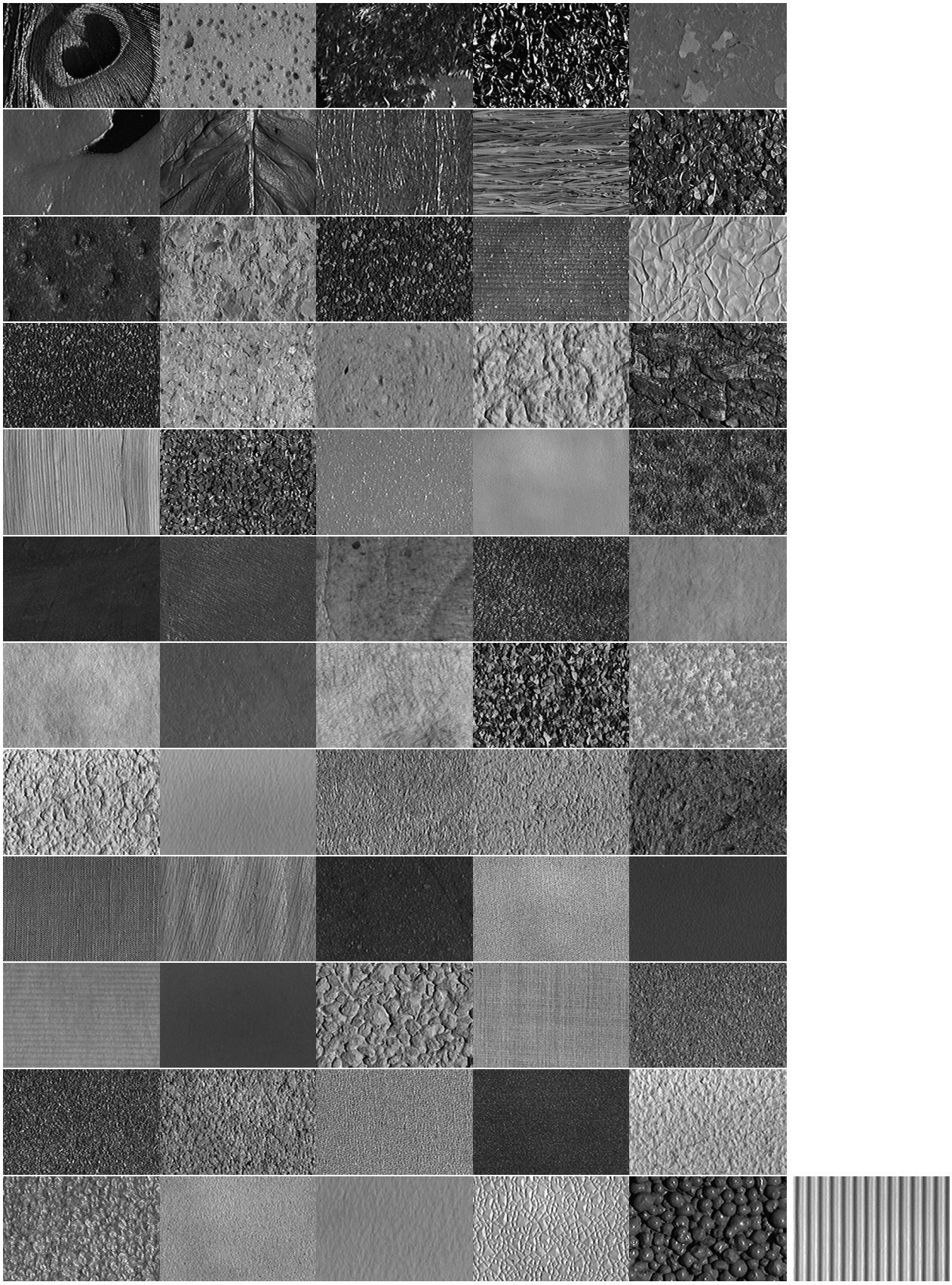

Fig. 2. The Curet dataset [9] sorted by horizontal fractal dimension $D_f(x)$.